Materials and Design 31 (2010) 2454–2463

Contents lists available at ScienceDirect

Materials and Design

journal homepage: www.elsevier.com/locate/matdes

Effect of process parameters on the strength of resistance spot welds in 6082-T6 aluminium alloy

A.M. Pereira [a,*], J.M. Ferreira [b], A. Loureiro [b], J.D.M. Costa [b], P.J. Bártolo [a]

[a] CDRsp, Centre for Rapid and Sustainable Product Development, Polytechnic Institute of Leiria, Morro do Lena – Alto Vieiro, 2400-901 Leiria, Portugal
[b] CEMUC, Centre of Mechanical Engineering of University of Coimbra, Rua Luís Reis dos Santos, Pólo II da Universidade de Coimbra, 3030-788 Coimbra, Portugal

ARTICLE INFO

Article history:
Received 24 September 2009
Accepted 21 November 2009
Available online 26 November 2009

Keywords:
Welding (D)
Mechanical properties (E)
Failure analysis (H)

ABSTRACT

In this study the microstructural and mechanical behaviour of resistance spot welds (RSW) done on aluminium alloy 6082-T6 sheets, welded at different welding parameters, is examined. Microstructural examinations and hardness evaluations were carried out in order to determine the influence of welding parameters on the quality of the welds. The welded joints were subjected to static tensile-shear tests in order to determine their strength and failure mode. The increase in weld current and duration increased the nugget size and the weld strength. Beyond a critical nugget diameter the failure mode changed from interfacial to pullout. Taking into consideration the sheet thickness and the mechanical properties of the weld, a simple model is proposed to predict the critical nugget diameter required to produce pull-out failure mode in undermatched welds in heat-treatable aluminium alloys.

1. Introduction

Resistance spot welding (RSW) is a process of joining metal components through the fusion of discrete spots at the interface of the work pieces. It is one of the most useful and practical methods for the manufacture of sheet metal assemblies [1]. This process is ideal for joining low carbon steel, stainless steel and nickel, aluminium or titanium alloy components and is thus used extensively [2–5]. This welding method can be used for the bodies and chassis of automobiles, trucks, trailers, buses, and railroad passenger cars, cabinets, office furniture and many other products.

Increasing restrictions in terms of performance, pollution, safety and energy consumption have resulted in research into the use of new materials and new processes aimed at weight reduction in the production of components and equipment. Improvements are obtained through lighter materials, like aluminium alloys and better joining processes, such as resistance spot welding [6,7].

One of the major advantages of RSW is the easy automation (high speed and adaptability) in high-volume production. Despite the obvious advantages of RSW this process has a major problem due to the inconsistent quality from weld to weld. The complexity introduced by many sources of variability complicates automation, reduces the quality of the weld and increases production costs [3]. Therefore, it is necessary to identify and control the parameters affecting the quality of the weld.

During spot welding, important changes occur in the mechanical and metallurgical properties of the spot welded areas. The investigation of these changes is very important for the safety and quality of the welded joints [1]. Both the squeezing time and the load applied on the electrodes prior to the transit of welding current have an important effect on mechanical properties due to their influence on current flow. In fact they ensure that the faying surfaces will be in contact with each other during welding [8]. Also the welding current and weld time significantly influence the properties of spot welds. In summary, the shear strength of single lap spot welded joints is a complex phenomenon, which depends on several factors, namely, welding parameters and base material properties. These factors control the microstructure and size of the weld nugget, which determine the mechanical behaviour of the welds [5,9,10]. The nugget is the melted region located in the interface between the abutting plates being welded.

In general an increase in weld current coarsens the microstructure of the weld nugget and heat-affected zone and affects the hardness, though the weld hardness is also very influenced by the base material's composition and state of treatment [5,9,11]. With austenitic stainless steel the increase in weld current does not produce any substantial change in the distribution of hardness within the nugget because it cannot be hardened by heat-treatment [5,10]. However, in heat or mechanically treated aluminium alloys, the increase in heat input during welding leads to a decrease in microhardness and strength in the welds [12].

An increase in weld current and heat input increased the nugget size and improved the failure load of spot welds done on carbon and stainless steels, aluminium and magnesium alloys

* Corresponding author. Tel.: +351 244820300; fax: +351 244820310.
E-mail address: mpereira@estg.ipleiria.pt (A.M. Pereira).

0261-3069/$ - see front matter © 2009 Elsevier Ltd. All rights reserved.
doi:10.1016/j.matdes.2009.11.052

[1,5,9,11,13,14]. However, the tensile-peel strength and tensile-shear strength reach a maximum with the weld current and decreases after this value [15]. This happens because the nugget diameter increases with current up to a specific value. After that value, the nugget diameter decreases because of excessive melting and splashing. This was observed by Vural et al. [16] for several material type combinations. The weld strength is also correlated with other process parameters, for example the applied load in welds carried out on stainless steel sheets [17].

The main failure modes for static weld strength tests using lap shear or cross tension samples are interfacial and nugget pull-out failure. Partial interfacial fracture is also observed [14,18]. In the interfacial mode, failure occurs via crack propagation through the nugget fusion zone (FZ), while, in pullout mode failure occurs via complete nugget withdrawal from one sheet. Partial interfacial fracture combines both modes of fracture. Welds that fail in nugget pullout mode provide higher peak loads and energy absorption levels than those which fail in interfacial failure mode. Because of this, process parameters should be adjusted so that pull-out failure mode is guaranteed [13,19], in order to ensure the reliability of the welds. In the early days of spot welding, the static strength of spot welds in steel was considered to be only dependent on the weld nugget size. Several equations were proposed to predict the optimum or the minimum nugget diameter to guarantee the pull-out failure mode of the welds. In Eq. (1), proposed by the American Welding Society/American National Standard Institute/Society of Automotive Engineers [20] for welds in steel, the critical nugget size d is simply function of the sheet thickness t, both in mm.

$$d = 4\sqrt{t} \tag{1}$$

However, several authors claim this equation is not safe for sheet thicknesses beyond 1.0–1.5 mm [19,21] and the alterations that occur in the mechanical properties of the weld should be taken into consideration. Eq. (2) was recommended by Pouranvari et al. [19] to predict the critical nugget diameter d_{cr}, and besides the sheet thickness t it considers the hardness of the failure line material $(H)_{FL}$ and of the nugget $(H)_{WN}$.

$$d_{cr} = 8t\frac{(H)_{FL}}{(H)_{WN}} \tag{2}$$

Those equations and others presented in the literature were mainly derived for welds in steels and few are mentioned for welds in aluminium alloys. Eq. (3) was proposed by Sun et al. [22] for welds in aluminium alloys 5182-O and 6111-T4, where no substantial change in hardness was observed in the welds. $D_{critical}$ is the critical size of the nugget required for pull-out failure, t the sheet thickness and f a porosity factor to consider influence of nugget porosity on the weld strength.

$$D_{critical} = \frac{3.2t}{f} \tag{3}$$

Though the effect of the process parameters on the mechanical behaviour of resistance spot welds on carbon and stainless steels is well documented results from aluminium alloys continue to be scarce. A better understanding of the effect of process parameters on the mechanical behaviour of spot welded joints in heat-treatable aluminium alloys such as 6082-T6 is still required. The objective of the current research is to investigate the effect of process parameters on shear strength and failure mode of spot welded joints in thin sheets of 6082-T6 aluminium alloy.

2. Experimental procedure

Aluminium alloy 6082-T6 sheets of 1 mm thick were used in this study. The nominal chemical composition and basic mechanical properties of this alloy are given in Table 1. Resistance spot welding lap joints were done on specimens of 100 mm × 25 mm × 1 mm in size. Fig. 1 shows the geometry and dimensions of the welded specimens. Sheet surfaces were randomly abraded with silicon carbide paper – P220 grade and afterwards cleaned with a dry air jet before resistance spot welding.

The welds were done using a Sciaky RSW type PMC02 electric resistance spot welding machine, with a nominal welding power of 100 kVA. The machine employs type C18200 electrodes having an end diameter of 15.25 mm, an electrical conductivity of 0.463 m/Ω mm^2 and a tensile strength of 310 N/mm^2. The hemispherical electrode tip radius is of 101.6 mm. The welding conditions were selected based on previous tests. Thirteen weld series were done, changing the weld current, time and electrode force. The timing diagram used in all tests is schematically represented in Fig. 2.

The variable welding parameters used for each series are given in Table 2. The squeeze and forge times were constant in all tests. The forge force used was 6474.6 N. The welds were done in open air at room temperature.

Five specimens were welded in each series; four specimens to be used for static tensile-shear strength testing and one for microstructure examination and hardness measurement. Specimens were examined by X-rays before testing in order to detect internal defects. Specimens used for microstructure examination and hardness measurement were cut out along the center of the nugget, at right angles to the longitudinal direction of specimens. Specimens were polished and a modified Poulton's reagent was employed to

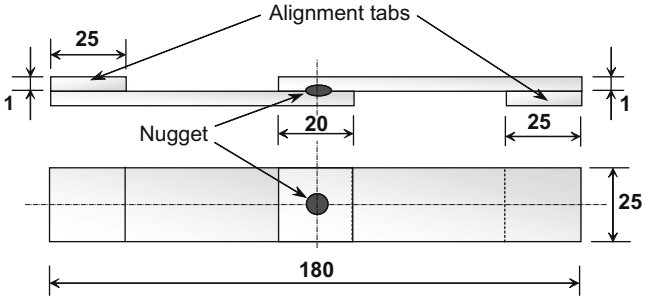

Fig. 1. Dimensions of tensile-shear test specimens (not to scale, dimensions in mm).

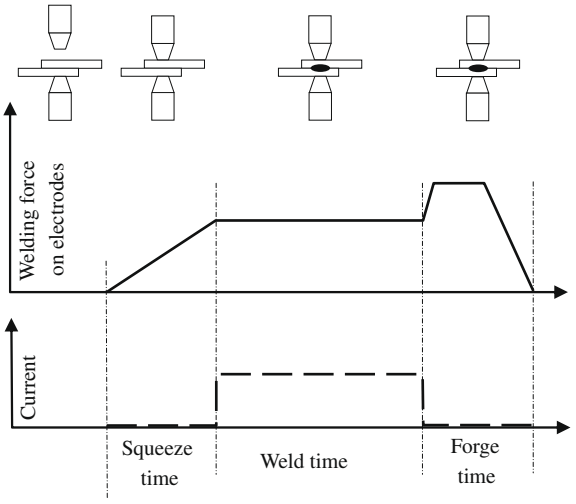

Fig. 2. Typical spot welding cycle.

Table 1
Chemical composition and mechanical properties of the 6082-T6 aluminium alloy.

Tensile strength (MPa)	Yield strength (MPa)	Alloying elements (wt.%)					
		Si	Mn	Mg	Fe	Cu	Al
305.6	245.1	1.02	0.67	0.76	0.26	0.02	97.24

Table 2
Resistance spot welding parameters used in each welds series.

Specimen series no.	Electrode force (N)	Weld time (cycles)	Weld current (kA)	Specimen series no.	Electrode force (N)	Weld time (cycles)	Weld current (kA)
1	3237	2	23.50	8	3237	5	26.40
2	3237	2	26.40	9	4709	2	26.40
3	3237	2	26.90	10	3826	2	26.40
4	3237	2	27.50	11	2649	2	26.40
5	3237	1	26.40	12	2354	2	26.40
6	3237	3	26.40	13	3237	2	28.70
7	3237	4	26.40				

reveal the microstructure. Metallographic analysis was performed using a ZEISS HD 100 optical microscope. Hardness measurements were carried out in two directions (along the radius of the nugget and through the sheet thickness) using a Struers Duramin Vickers machine, under a load of 100 g. The shear strength testing was done in an electromechanical Instron Universal Testing machine at a constant cross-head speed of 1 mm/min, up to the final failure of the joint.

3. Results and discussion

3.1. Weld morphology

The resistance spot welds were of excellent visual appearance for the entire range of parameters tested, though it was apparent that there was variation in spot diameter and spot indentation depth with the change of the process parameters. Radiographic inspection showed the welds were free of internal defects, such as pores or voids. Subsequent metallographic analysis was used to measure the correct dimensional characteristics of the welds, mainly the size of the weld nugget, and to characterize the microstructure, as well to confirm that welds were completely free of defects, see Fig. 3. This subject is very important because several authors [22,23] mentioned that the presence of porosity affects the strength of spot welds in aluminium alloys. Nugget diameter was largely influenced by the weld current and current flow time.

The effect of the variation of weld current and time on nugget diameter is shown in Figs. 4 and 6. The nugget diameter increases continuously with weld current up to the maximum intensity tested, see Fig. 4. This behaviour can be attributed to the increase in heat input with increasing current and it agrees well with results observed by other authors in welds in carbon steels [19]. Most of the authors doing research in steels mention that there is a current threshold above which the nugget diameter decreases due to splash phenomena [14]. The results obtained suggest that the current threshold for the applied electrode force was not reached, because though little splash was produced at the current of 28.7 kA no reduction in the nugget diameter was observed, as shown in Fig. 4. According to several authors, the weld current can be increased without expulsion of melted material by increasing electrode force [24,25]. Metallographic analysis will show the appearance of incomplete expulsion for high weld currents. However, the welding current also affects weld indentation. In fact, all the welds display some indentation, which is largely influenced by the welding current, as illustrated in Fig. 5.The indentation is represented in this graph by the reduction in percentage of the initial thickness of the plates. A sudden increase in the reduction of plate thickness was observed for weld currents above 27 kA. Under this value the indentation seems to be unaffected by current level.

The increase in weld time results in increasing nugget diameter only up to a weld time of 3 cycles, see Fig. 6. After this time the nugget diameter seems to remain unchanged. However, the results obtained in RSW of steels show that there is a decrease in the nugget size after a critical weld time [14]. It is interesting to mention that though the nugget size remains approximately constant for current times beyond 3 cycles weld indentation continues to increase with time, as illustrated in Fig. 7, because of the increase in the global heat input.

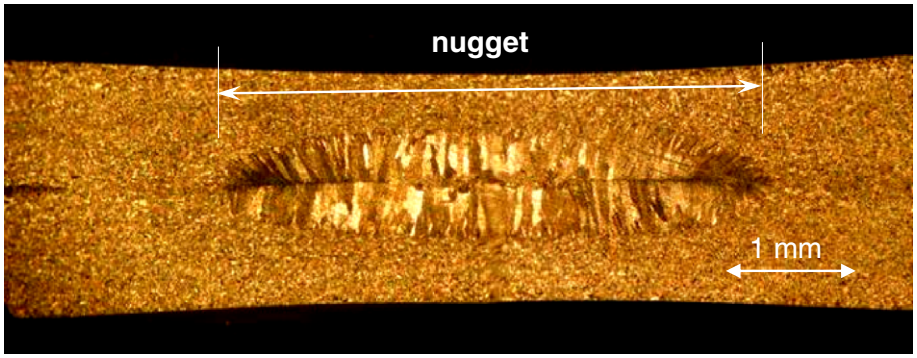

Fig. 3. Macrostructure of a RSW nugget (23.5 kA; 2 cycles; 3237 N).

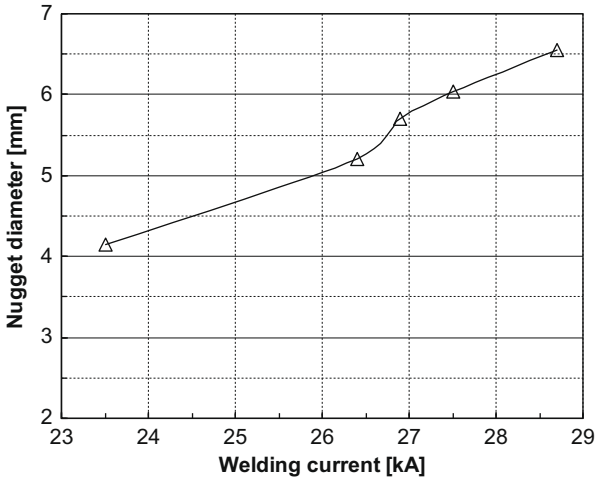

Fig. 4. Welding current versus nugget diameter (2 cycles; 3237 N).

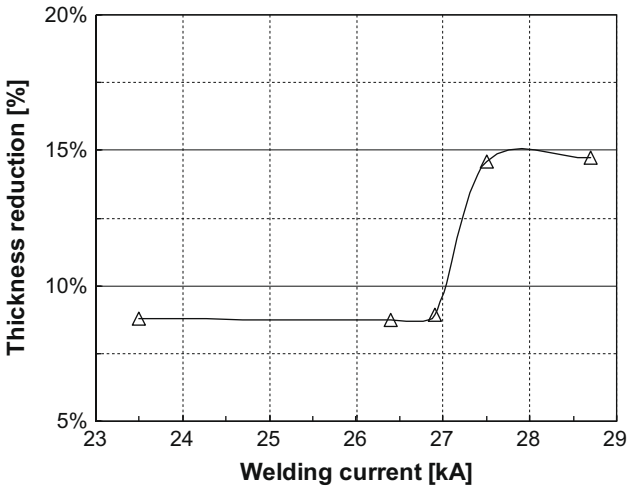

Fig. 5. Welding current versus thickness reduction (2 cycles; 3237 N).

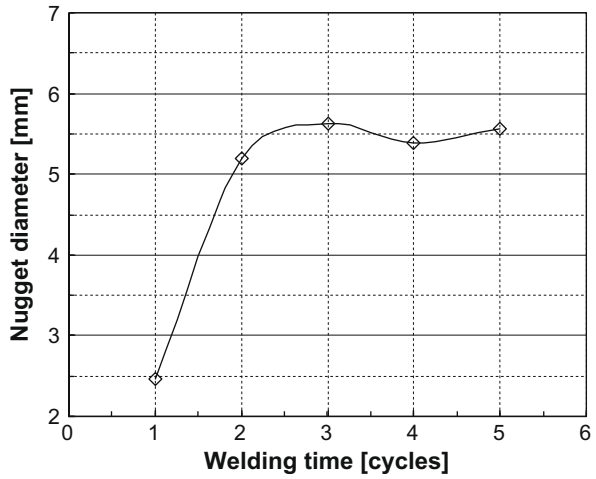

Fig. 6. Welding time versus nugget diameter (26.4 kA; 3237 N).

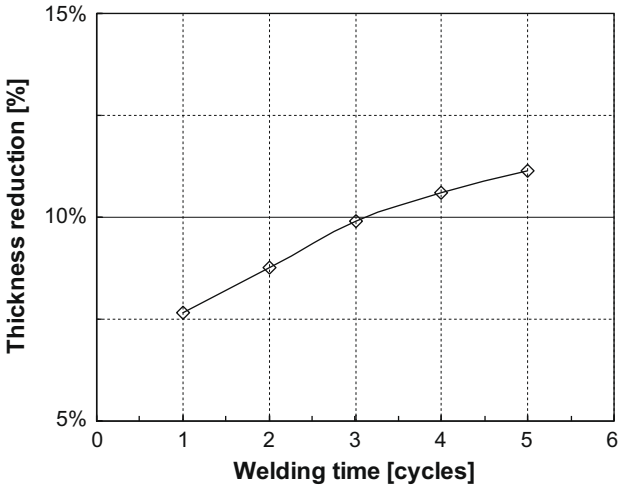

Fig. 7. Welding time versus thickness reduction (26.4 kA; 3237 N).

The electrode force does not significantly affect the nugget size for loads up to approximately 4000 N, though above this value some reduction in nugget diameter was observed, as shown in Fig. 8. The explanation for this may be that the increase in the electrode force above that value can significantly improve the contact between the faying surfaces, decreasing electrical resistance and heat input. Other authors agree that the evolution of the weld nugget size with electrode load is largely dependent on the interfacial contact of the plates [19,24]. The electrode force showed a minor effect on the indentation depth in the range of electrode forces tested. The effect of the electrode force on the thickness reduction was analysed in detail for an intermediate current of 26.4 kA and time of 2 cycles, in a range of loads between 2354 and 4709 N. The electrode force showed a minor effect on the indentation depth, displaying all the welds a thickness reduction around 10%.

3.2. Microstructure

The resistance spot welding process is a thermal, metallurgical and mechanical deformation process that results in a melted region, currently named the nugget, and a heat-affected zone around the nugget. The size and type of microstructures in these regions is considerably affected by the heat input in the process. The

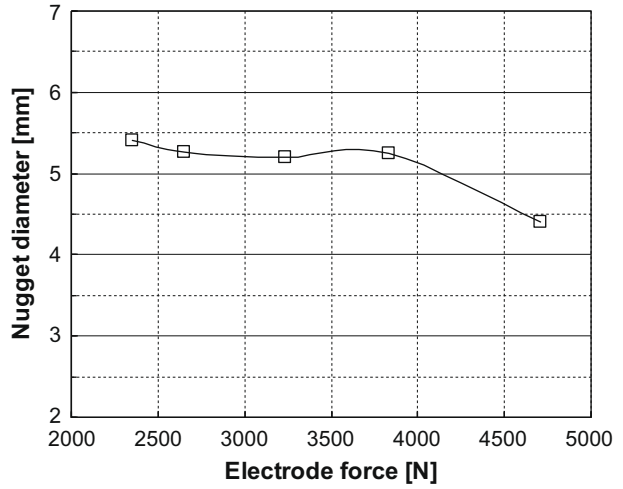

Fig. 8. Electrode force versus nugget diameter (26.4 kA; 2 cycles).

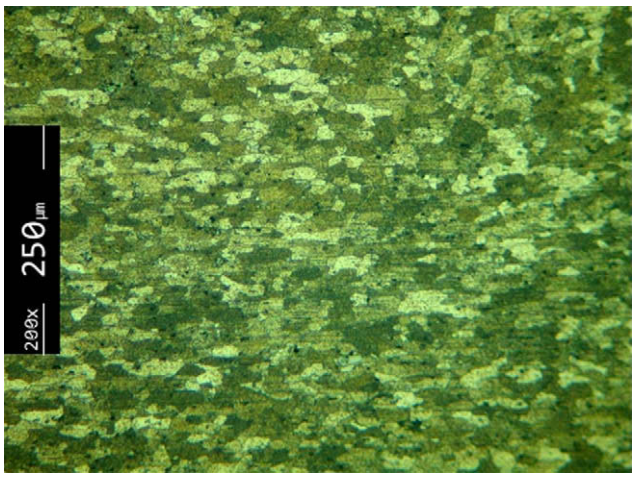

Fig. 9. Microstructure of the aluminium alloy 6082-T6 sheets.

microstructures of the weld nugget are quite different from those of the base material. The microstructure of the base material is illustrated in Fig. 9. The microstructure consists mainly of pancake shaped grains, elongated in the rolling direction, as shown in the central part of the figure, though some equiaxed grains coexist in the structure.

The microstructure of the weld nugget is dominated by a columnar structure oriented in the direction of heat flow. This microstructure is greatly affected by welding parameters, mainly weld current and current flow time.

Figs. 10 and 11 illustrate the microstructures of the nugget of welds done using 23.5 kA and 28.7 kA, both for 2 cycles of current flow time and with 3237 N of electrode force.

A columnar structure, with a segregation zone in the region corresponding to the faying surface, was observed in the nugget of welds done using the lowest current, as illustrated in Fig. 10. The segregation zone in the nugget is more enhanced in welds done using lower welding currents.

A significant coarsening of the columnar structure was observed in the nugget of welds done using increasing weld current, as shown in Fig. 11. In addition, some equiaxed grains form in the centre of the nugget, suggesting a lower cooling rate and thermal gradient in the welds. Some grain coarsening was also observed in the heat-affected zone of welds carried out with high weld current.

The metallographic study also revealed that for high current levels an incipient flash occurs in the faying surfaces, though metal projections were not apparent during welding. Fig. 12 illustrates the premature expulsion of melted material from the nugget. In fact the melted material cools before reaching the edge of the welded plates. These metal projections only happened for weld currents above 27.5 kA.

3.3. Hardness

Fig. 13 illustrates the effect of the weld current on the hardness distribution in the welds. A narrow range of currents was used because for a 1 mm thick plate a current value under 23.5 kA does not give adequate welds and above 28.7 kA causes projections of material during welding. The gray ribbon in the following figures represents the hardness of the base material. A significant decrease in hardness was observed in the nugget of all the welds. The reduction in hardness of the nugget is quite similar for all weld currents used. This decrease in hardness is currently attributed to the dissolution

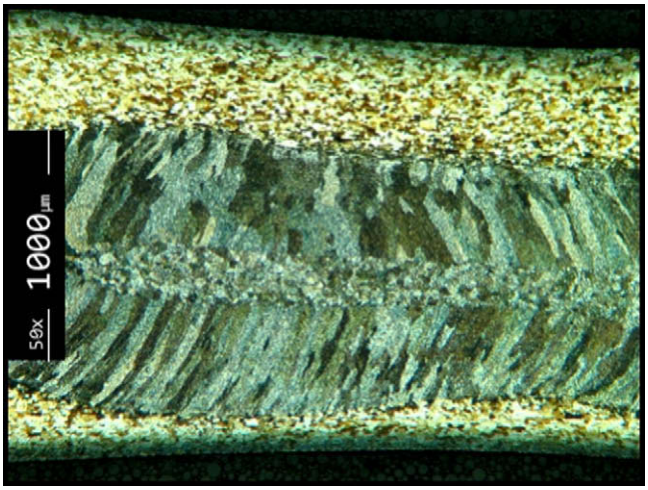

Fig. 11. Microstructure of the nugget of a welded joint done at 28.7 kA; 2 cycles; 3237 N.

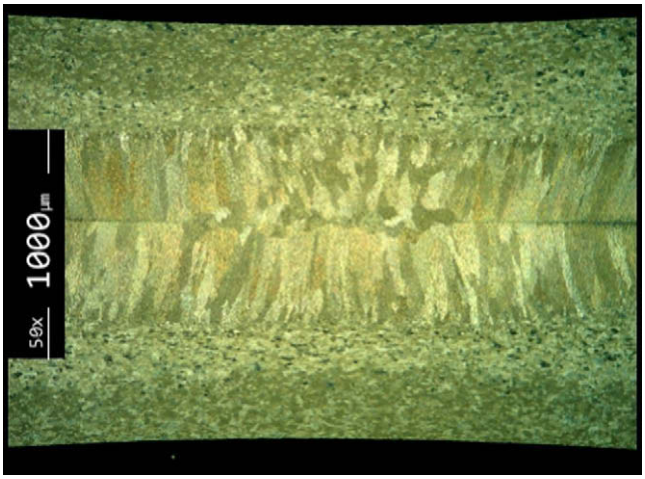

Fig. 10. Microstructure of the nugget of a weld done using 23.5 kA; 2 cycles; 3237 N.

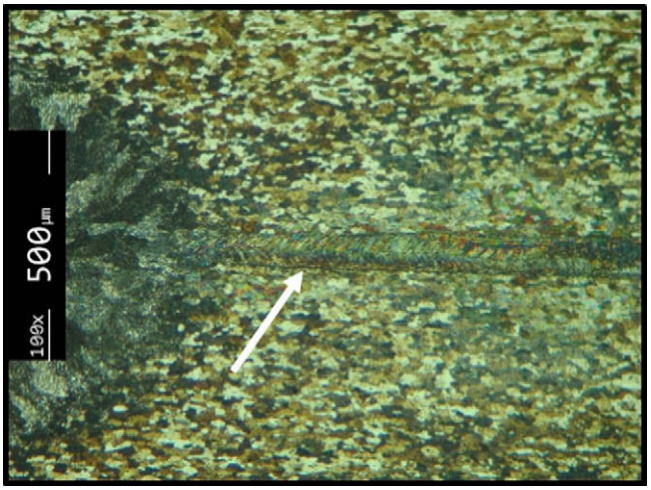

Fig. 12. Premature expulsion of melted material from the nugget of a welded joint done at 28.7 kA, 2 cycles and 3237 N.

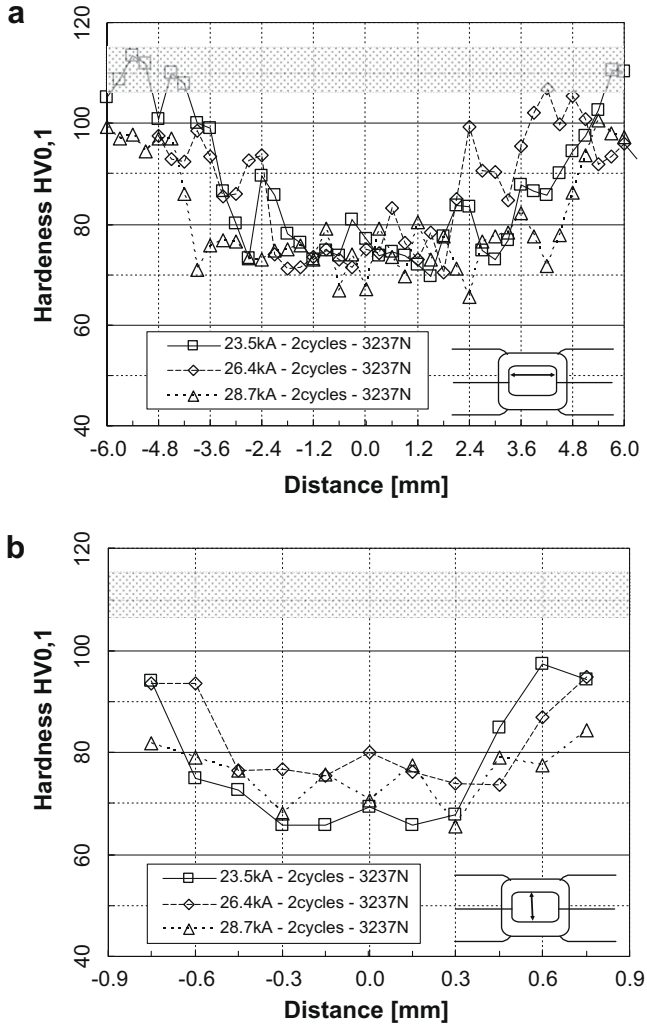

Fig. 13. Influence of weld current on hardness plot in: (a) transversal line and (b) through thickness line (2 cycles; 3237 N).

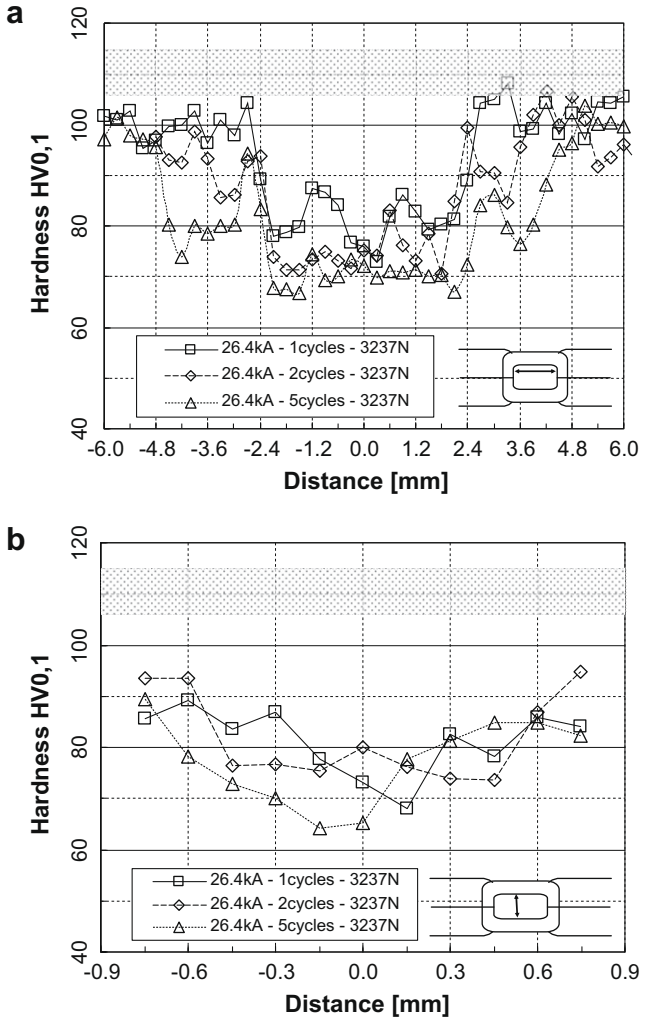

Fig. 14. Influence of weld time on hardness plot in: (a) transversal line and (b) through thickness line (26.4 kA; 3237 N).

of strengthening precipitates in welds in 6xxx aluminium alloys, mainly in the T6 state [26,27]. These results show that the precipitates were solubilised, even for the lowest current level. The variation of weld current influences mainly the width of the zone affected by the heat generated in the process, as is shown in Fig. 13a. This is because increasing weld current increases the nugget size, as mentioned above, and also the width of the *HAZ*.

Through thickness hardness measurements, see Fig. 13b, show that the decrease in hardness is concentrated principally in the nugget, where the highest temperatures during welding were reached, though the regions close to the plates' surface, the *HAZ*s, also undergo some reduction in hardness.

The effect of the weld time on hardness distribution through the cross section of welds, in the transverse and through-thickness directions, is illustrated in Fig. 14a and b. The effect of the weld time is similar to the influence of the weld current. The decrease in hardness is a little more pronounced in welds done using 5 cycles than in single cycle welds, see Fig. 14a. These results suggest that the increase in weld time augmented the heat input, consequently increasing the dissolution of the strengthening precipitates. The substantial decrease in hardness observed on both sides of the nugget in the heat-affected zone, though not as stressed as in the nugget, tends also to extend to a larger distance in welds done with five weld cycles. The coarsening of precipitates is usually mentioned as the main reason for the softening of the structure in the heat-affected zone [28].

The softening effect was also observed through the entire thickness of the sheets, as shown in Fig. 14b, where the hardness of the base material is illustrated by a grey bar. The largest reduction in hardness was observed in the nugget of the welds, where the melting of the base materials promoted the total dissolution of the strengthening precipitates.

The effect of the electrode force on the distribution of hardness in the welds is illustrated in Fig. 15a in transverse direction and through-thickness in Fig. 15b. A slight effect of electrode force on hardness distribution was observed in both directions.

3.4. Peak load and failure mode

It is currently assumed that the mechanical strength of the RSW is mainly influenced by the nugget diameter, though several authors [19,22] admit that the mechanical properties of the nugget and *HAZ* of the welds, where weld failures happen, also play a relevant role in the performance of the welds. Both nugget size and mechanical properties of the welds are directly affected by the welding parameters, such as welding current, welding time and electrode force, as shown in previous sections. Fig. 16 illustrates the effect of these parameters on the failure load of the welds.

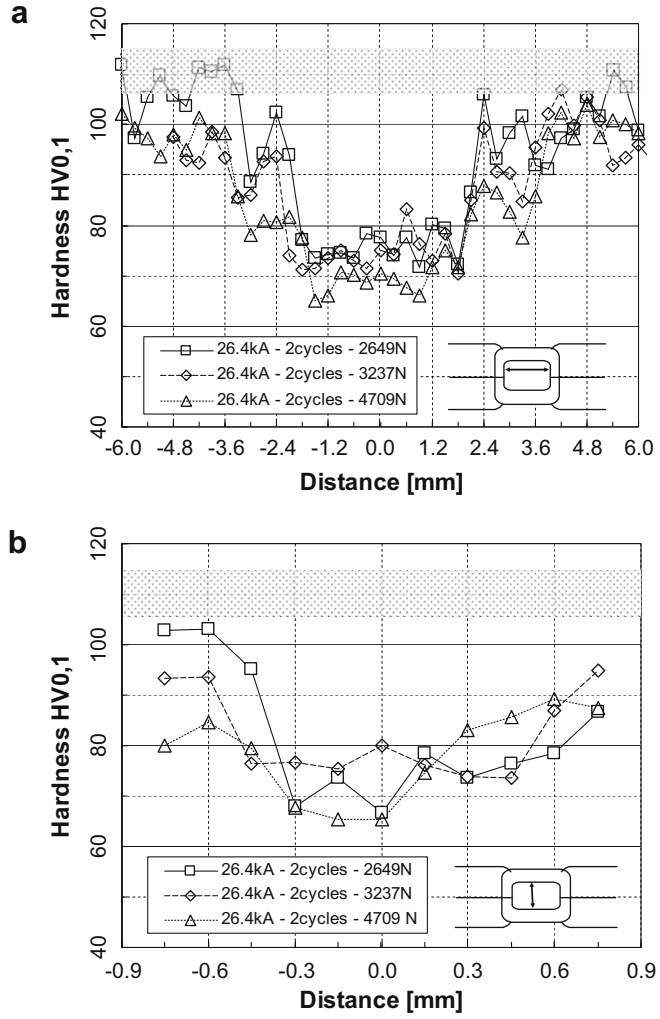

Fig. 15. Influence of the electrode force on the hardness plot in: (a) transversal line and (b) through thickness line (26.4 kA; 2 cycles).

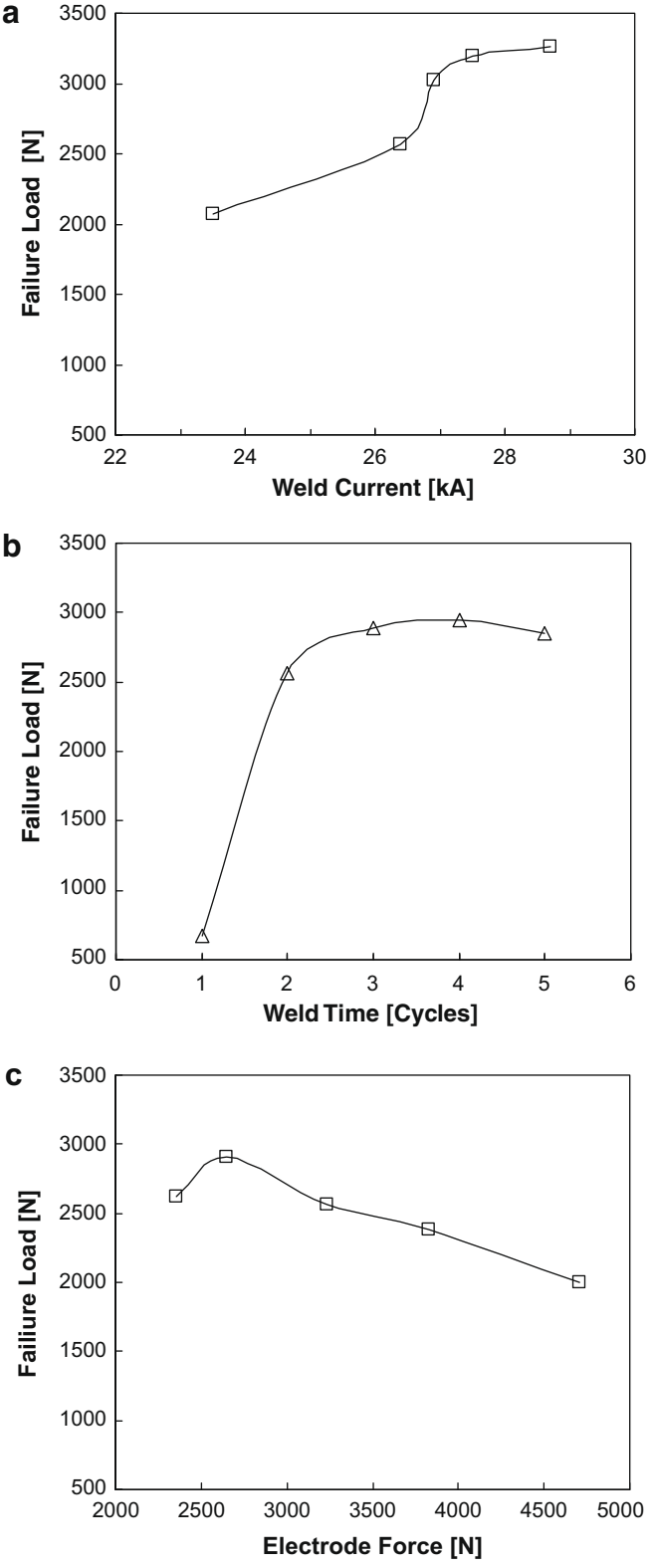

Fig. 16. Failure load versus the variation of: (a) current welding (weld time: 2 cycles and force on electrode: 3234 N); (b) weld time (weld current: 26.4 kA and force on electrode: 3234 N) and (c) electrode force (weld time: 2 cycles and weld current: 26.4 kA).

The influence of the weld current on the failure load is illustrated in Fig. 16a. A significant increase in the failure load with increasing weld current was observed, even for the maximum current studied (28.7 kA), where one small expulsion of material occurred. The reason for this behaviour is that the increase in current augmented the nugget diameter, as shown in Fig. 4.

The effect of the weld time on the failure load is shown in Fig. 16b. A significant increase in the failure load was observed with increasing weld time. This effect is caused by the increase in the nugget diameter with weld time, as shown in Fig. 6. Above 2 cycles weld time neither the nugget size nor the peak load increase. The welding parameters and consequent nugget diameter influence both the failure load and the failure mode. For example, the welds performed with two or more weld cycles presented pull-out failure mode, see Fig. 17a, as opposed to the welds done using a single weld cycle, which experienced an interfacial fracture, as is illustrated in Fig. 17b.

The influence of the electrode force on the failure load of the spot welds is illustrated in Fig. 16c. Generally, a small decrease in the failure load was observed with increasing electrode force. This reduction is associated with the decrease in the diameter of the nugget with increasing electrode force. The nugget diameter decreased from 5.3 mm to 4.4 mm with the increase in the electrode force from 2649 N to 4709 N.

The effect of weld parameters on failure load is quite similar to the influence of the same weld parameters on nugget diameter. This is not surprising because the mechanical properties of the

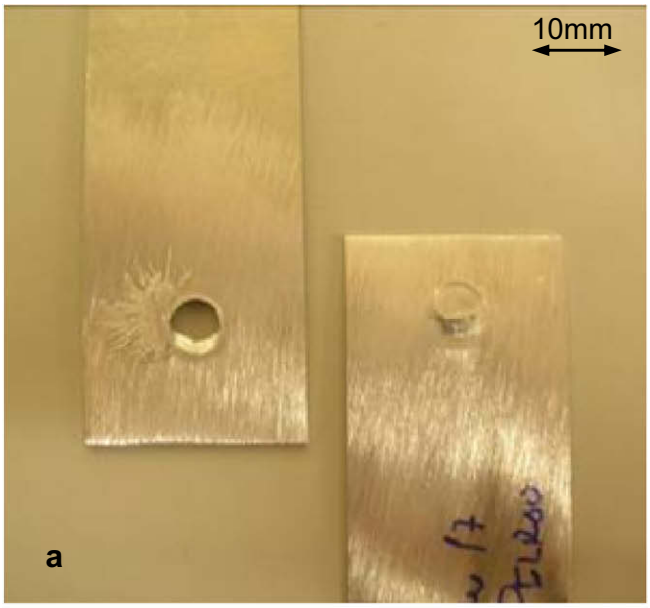

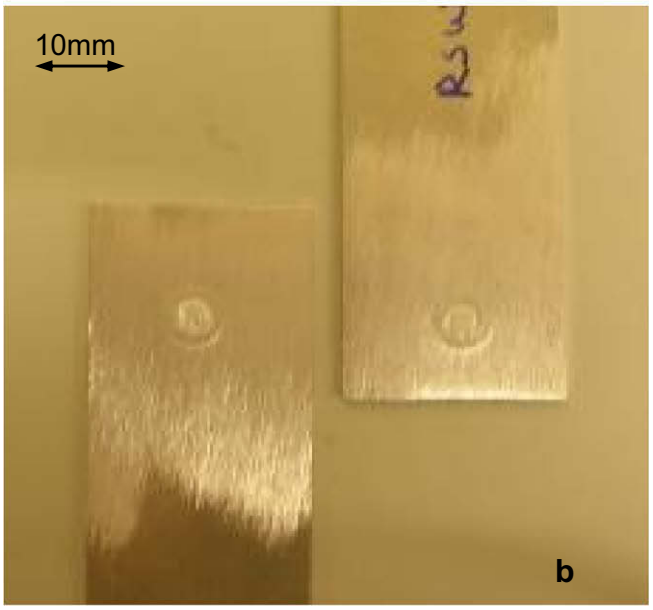

Fig. 17. RSW failure modes: (a) pull out mode and (b) Interfacial mode.

welds do not change significantly among the variety of the weld parameters studied, as is suggested by the evolution of the hardness, see Figs. 14–16. In fact the decrease in hardness is quite similar, mainly in the nugget area, for all weld conditions.

Fig. 18 shows the relationship between the weld nugget diameter and the fracture peak load, from the results of the static lap shear tests. An approximately linear relationship was observed between nugget diameter and failure load. The failure modes observed in the tests are also illustrated in the same graph. The interfacial failure mode is denoted by open lozenges, and the pull-out failure mode by open triangles. The separation between the zones of preferential interfacial failure and pull-out failure modes is indicated in Fig. 18 by dotted lines. The interfacial failure mode occurs for nugget diameters up to 5.1 mm while pull-out failure mode happened for nugget diameters above 5.6 mm. For nugget sizes between 5.1 and 5.6 mm both modes of failure coexist.

Currently, in order to guarantee the reliability of the welds, the welding parameters should be adjusted so that pull-out failure

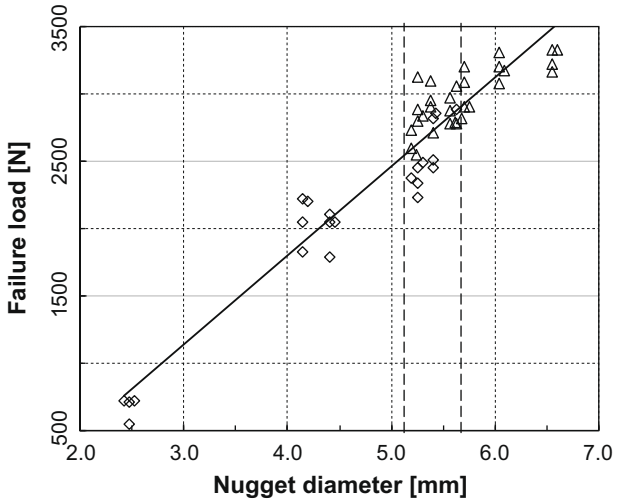

Fig. 18. Effect of weld nugget size on peak load and failure mode (◇ – interfacial failure mode; Δ – pull-out failure mode).

mode is obtained during testing. The equation proposed by AWS/SAE/ANSI [20,29], Eq. (1), developed specifically to predict the critical nugget diameter to guarantee the pull-out failure mode in welds in steels, is not reliable for welds in aluminium because it recommends a nugget diameter of 4 mm to get pull-out failure, instead of the value of 5.6 mm, observed in this investigation. Even the formulas used in the automotive industry [29] give only 4.2 and 5.3 mm, respectively, for minimum and nominal nugget diameter. It also seems that the formulas proposed by Chao [21] are not applicable because they are based on the stress intensity factor which has no meaning in the case of ductile materials, such as those studied in the present investigation.

On the other hand the equation proposed by Pouranvary et al. [19], Eq. (2), is too conservative, giving critical nugget diameters of 8 mm or more, because in heat-treatable aluminium alloys the hardness of the *HAZ* is similar or superior to the hardness of the nugget.

The equation suggested by Sun et al. [22], Eq. (3), predicts nugget diameters that are too small, 3.2 mm in this case, because it was derived for welds in 5xxx and 6xxx aluminium alloys, where almost no softening or hardening happens, and not for heat-treatable aluminium alloys in the T6 state.

As none of the analytical models mentioned above seems adequate to describe the mechanical behaviour of resistance spot welds in heat-treatable aluminium alloys subjected to shear lap tensile testing, a simple analytical model was derived to predict the critical spot weld diameter required for pull-out failure mode. Like the previous models, this one assumes the failure is a competitive process where the failure happens in the weakest weld zone; the nugget or the *HAZ*. The equation governing the interfacial failure of the nugget can be established assuming that shear is the dominant loading mode in shear tensile test. This is plausible because only incipient bending of the specimens occurs before interfacial weld failure. Furthermore, Pouranvari et al. [19] have already suggested this mechanism exists in shear tensile tests of spot welds. Therefore, assuming the shear stress is distributed uniformly in the cross section of the nugget, the interfacial failure load can be expressed by Eq. (4), where d is the nugget diameter and τ_N is the shear strength of the nugget.

$$L_{Int} = \frac{\pi d^2}{4}\tau_N \tag{4}$$

On the other hand, when pull-out failure occurs a significant bending of specimens was observed before failure during shear tensile test, suggesting a loading mode similar to that typical of

cross tension tests. In this case several authors consider that the failure mechanism is through-thickness shear in the *HAZ* [22,30]. In this case Eq. (5) can be considered to be the governing law for predicting pull-out failure load, L_{PO}. The nugget diameter is designated by d, the plate thickness by t and the shear strength of the *HAZ* by τ_{HAZ}.

$$L_{PO} = \pi d t \tau_{HAZ} \tag{5}$$

Therefore, the critical nugget diameter required to obtain pull-out failure (d_{cr}) is governed by Eq. (6), which results from the intersection of Eqs. (4) and (5).

$$d_{cr} = 4t\frac{\tau_{HAZ}}{\tau_N} \tag{6}$$

For spot welds with nugget diameters below d_{cr} the interfacial failure mode will be dominant while for diameters above this value spot welds will exhibit pull-out failure mode. However, the evaluation of the shear strength of the nugget and *HAZ* of spot welds is difficult, because those regions are narrow and present microstructural gradients. Currently, the yield and tensile strength of materials are related to their hardness through empiric equations characterised by the generic Eq. (7), where HV and σ represent the Vickers hardness and tensile strength of the material and K is approximately constant, assuming the elastic properties are approximately constant inside each family of materials [31,32]. In addition, according to the Tresca criterion, both the shear and tensile strength of a metal are connected by a mathematical constant, shear strength is half of the tensile strength of the material.

$$HV = K\sigma \tag{7}$$

Therefore, Eq. (6) can be rewritten as Eq. (8), where HV_N and HV_{HAZ} are the hardness of the nugget and *HAZ*.

$$d_{cr} = 4t\frac{HV_{HAZ}}{HV_N} \tag{8}$$

Hardness is easier to evaluate than the tensile strength of the nugget or *HAZ* of the welds, though a difficulty remains. While the hardness in the nugget is approximately constant and easy to average, the *HAZ*' hardness exhibits a gradient between the nugget and the non-affected base material, as shown in Figs. 14–16. Consequently d_{cr} is function of the chosen hardness of the *HAZ*. To give an example; Fig. 18 shows that the minimum required diameter to get consistent pull-out failures is 5.6 mm. This corresponds to welds done using 26.4 kA, 2 cycles and 3237 N as welding parameters. One example of the evolution of the hardness in those welds is shown in Fig. 13. The average hardness in the nugget is HV75 and in the *HAZ* it is approximately HV95. Introducing those values in Eq. (8), the critical nugget diameter to get pull-out failures is given as 5.1, which corresponds to the lower limit for which pull-out failure can occur; though at that size interfacial failures can also occur, as shown in Fig. 18. As the definition of the average hardness in the *HAZ* is difficult, because of the hardness gradient, a safe critical diameter can be defined based on the hardness of the parent material instead of the hardness of the *HAZ*. In this case the new formulation of Eq. (8) is indicated in Eq. (9), where HV_{BM} is the hardness of the base material.

$$d_{cr} = 4t\frac{HV_{BM}}{HV_N} \tag{9}$$

For a base material hardness of HV110 the critical diameter calculated by Eq. (9) is 5.9 mm, very close the experimental observations. Eq. (9) allows us to define a safe boundary for obtaining pull-out failure, and has the advantage that the experimental values of HV_{BM} and HV_N can be evaluated in a quick and easy way. This model needs to be extended to RS welds in other aluminium sheet thicknesses. It was derived specifically for undermatched welds in heat-treatable aluminium alloys. The matching grade of welds is defined by the rate between the yield or tensile strength of the weld and the base material. According to whether this rate is equal to one, lower than one or higher than one the welds are considered to be in the evenmatch, undermatch or overmatch condition, respectively. In the present model, when the grade of undermatch increases, the critical nugget diameter increases too, in order to guarantee pull-out failure mode. For welds in mild steels, where the evenmatch condition is approximately observed, Eq. (9) gives higher critical nugget diameters than Eq. (1), of the American Welding Society et al. [20,29]. However Eq. (9) is not valid for overmatch welds, typical of RSW in high strength steels, because it gives unsafe nugget diameters.

4. Conclusions

The influence of the weld parameters on the microstructure and tensile-shear strength of resistance spot welds on an aluminium alloy 6082-T6 was studied. The conclusions obtained are summarised as follows:

- The increase in the weld current and time increased the nugget diameter and coarsened the microstructure; these transformations were accompanied by a significant decrease in hardness in the nugget and heat-affected zones of the welds.
- A significant increase in the failure load in static shear lap tests was observed in welds done with increasing weld current and time, because of the augmentation of the nugget diameter; beyond a critical nugget diameter the failure changes from interfacial mode to pullout mode.
- A simple analytical model was proposed to predict the critical nugget size to obtain pull-out failures in undermatched welds in heat-treatable aluminium alloys.

Acknowledgements

The authors thank the financial support of the Portuguese Foundation for Science and Technology (Grant SFRH/BD/37384/2007) and the assistance of the company OGMA-Indústria Aeronáutica de Portugal in the execution of the welds.

References

[1] Vural M, Akkus A. On the resistance spot weldability of galvanized interstitial free steel sheets with austenitic stainless steel sheets. J Mater Process Technol 2004;153–154:1–6.
[2] Kahraman N. The influence of welding parameters on the joint strength of resistance spot-welded titanium sheets. Mater Des 2007;28:420–7.
[3] Jou M. Real time monitoring weld quality of resistance spot welding for the fabrication of sheet metal assemblies. J Mater Process Technol 2003;132:102–13.
[4] Aslanlar S, Ogur A, Ozsarac U, Ilhan E, Demir Z. Effect of welding current on mechanical properties of galvanized chromized steel sheets in electrical resistance spot welding. Mater Des 2007;28:2–7.
[5] Özyürek D. An effect of weld current and weld atmosphere on the resistance spot weldability of 304L austenitic stainless steel. Mater Des 2008;29:503–97.
[6] Barnes TA, Pashby IR. Joining techniques for aluminium space frames used in automobiles part II – adhesive bonding and mechanical fasteners. J Mater Process Technol 2000;99:72–9.
[7] Pereira AM, Ferreira JM, Antunes FV, Bártolo PJ. Study on the fatigue strength of AA 6082 – T6 adhesive lap joints. Int J Adhes Adhes 2009;29.
[8] Santos IO, Zang W, Gonçalves VM, Bay N, Martins PAF. Weld bonding of stainless steel. Int J Mach Tools Manuf 2004;44:1431–9.
[9] Darwish SM, Al-Dekhial SD. Micro-hardness of spot welded (B.S. 1050) commercial aluminium as correlated with welding variables and strength attributes. J Mater Process Technol 1999;91:43–51.
[10] Shamsul JB, Hisyam MM. Study of spot welding of austenitic stainless steel type 304. J Appl Sci Res 2007;3(11):1494–9.
[11] Sun DQ, Lang B, Sun DX, Li JB. Microstructures and mechanical properties of resistance spot welded magnesium alloy joints. Mater Sci Eng A 2007;460–461:494–8.

[12] Leal RM, Loureiro A. Effect of overlapping friction stir welding passes in the quality of welds of aluminium alloys. Mater Des 2008;29:982–91.
[13] Marashi P, Pouranvari M, Amirabdollahian S, Abedi A, Goodarzi M. Microstructure and failure behavior of dissimilar resistance spot welds between low carbon galvanized and austenitic stainless steels. Mater Sci Eng A 2008;480:175–80.
[14] Goodarzi M, Marashib SPH, Pouranvari M. Dependence of overload performance on weld attributes for resistance spot welded galvanized low carbon steel. J Mater Process Technol 2009;209:4379–84.
[15] Aslanlar S. The effect of nucleus size on mechanical properties in electrical resistance spot welding of sheets used in automotive industry. Mater Des 2006;27:125–31.
[16] Vural M, Akkus A, Eryürek B. Effect of welding nugget diameter on the fatigue strength of the resistance spot welded joints of different steel sheets. J Mater Process Technol 2006;176:127–32.
[17] Bouyousfi B, Sahraoui T, Guessasma S, Chaouch KT. Effect of process parameters on the physical characteristics of spot weld joints. Mater Des 2007;28:414–9.
[18] Sun X, Stephens EV, Khaleel MA. Effects of fusion zone size and failure mode on peak load and energy absorption of advanced high strength steel spot welds under lap shear loading conditions. Eng Fail Anal 2008;15:356–67.
[19] Pouranvari M, Asgari HR, Mosavizadeh SM, Marashi PH, Goodarzi M. Effect of weld nugget size on overload failure mode of resistance spot welds. Sci Technol Weld Join 2007;12:217–25.
[20] Weld button criteria, recommended practices for test methods for evaluating the resistance spot welding behavior of automotive sheet steel metal, American National Standard. ANSI/AWS/SAE/D8.9-97. Section 5.7; 1997.
[21] Chao YJ. Failure mode of resistance spot welds: interfacial versus pullout. Sci Technol Weld Join 2003;8:133–7.
[22] Sun X, Stephens EV, Davies RW, Khaleel MA, Spinella DJ. Effects of fusion zone size on failure modes and static strength o aluminum resistance spot welds. Weld J 2004;83(11):308s–18s.
[23] Chuco W, Gould J. Metallurgical interpretation of electrode life in resistance spot welding of aluminum sheet. In: Proceedings of joining of advanced and specialty materials. St. Louis (Mo): ASM International; October 9–11 2000. p. 114–21.
[24] Browne DJ, Chandler HW, Evans HW, Wen J. Computer simulation of resistance spot welding in aluminum: Part 1. Weld J 1995;74(10):339s–44s.
[25] Browne DJ, Chandler HW, Evans HW, Wen J, Newton CJ. Computer simulation of resistance spot welding in aluminum: Part 2. Weld J 1995;74(12):417s–22s.
[26] Starink MJ, Deschamps A, Wang SC. The strength of friction stir welded and friction stir processed aluminium alloys. Scripta Mater 2008;58:377–82.
[27] Simar A, Bréchet Y, de Meester B, Denquin A, Pardoen T. Microstructure, local and global mechanical properties of friction stir welds in aluminium alloy 6005A-T6. Mater Sci Eng A 2008;486:85–95.
[28] Heinz B, Skrotzki B. Characterization of a friction-stir-welded aluminium alloy 6013. Metall Mater Trans B 2002;33B(June):489–98.
[29] Ewing KW, Cheresh M, Thompson R, Kukuchek P. 'Static and impact strengths of spot-welded HSLA and low carbon steel joints' SAE 820281. Warrendale (PA): Society of Automotive Engineers; 1982.
[30] Lin SH, Pan J, Wu SR, Tyan T, Wung P. Failure loads of spot welds under combined opening and shear static loading conditions. Int J Solids Struct 2002:3919–39.
[31] Salazar-Guapuriche MA, Zhao YY, Pitman A, Greene A. Correlation of strength with hardness and electrical conductivity for aluminium alloy 7010. Mater Sci Forum 2006;519–521:853–8.
[32] Busby JT, Hash MC, Was GS. The relationship between hardness and yield stress in irradiated austenitic and ferritic steels. J Nucl Mater 2005;336:267–78.